M-shell x-ray-production cross sections in thin targets of $_{79}$Au, $_{82}$Pb, $_{83}$Bi, and $_{92}$U by 0.3–2.6-MeV $^{1}_{1}H^{+}$ and $^{4}_{2}He^{+}$ ions

R. Mehta, J. L. Duggan, J. L. Price, and F. D. McDaniel
Department of Physics, North Texas State University, Denton, Texas 76203

G. Lapicki
Department of Physics, East Carolina University, Greenville, North Carolina 27834
(Received 11 May 1982)

M-shell x-ray-production cross sections are reported for $^{1}_{1}H^{+}$ and $^{4}_{2}He^{+}$ ions incident on thin targets of $_{79}$Au, $_{82}$Pb, $_{83}$Bi, and $_{92}$U. The energy of the ions ranged from 0.3 to 2.6 MeV in increments of 0.1 MeV. The first Born calculations overpredict the data at all energies studied. The perturbed-stationary-state calculations with energy loss, Coulomb deflection, and relativistic effects agree with the present data for both $^{1}_{1}H^{+}$ and $^{4}_{2}He^{+}$ ions at $\sim$0.35 MeV/u, overpredict the data at higher E_1/A_1, and underpredict the data at lower E_1/A_1. The electron-capture contribution to the target ionization is calculated to be less than 3.4% for the targets, projectiles, and energies reported in this work.

INTRODUCTION

In the last decade there have been numerous studies of x-ray-production cross sections for ion-atom collisions in the MeV energy region. These cross sections have been shown to be important in practical applications such as trace analysis,[1,2] ion implantation,[3–5] and fusion diagnostic studies.[6,7] The theoretical models have shown, in general, to be in good agreement with the experimental measurements. A glance at the articles published last year in this journal reveals that most of the previous work has been limited to K- and L-shell measurements of the cross sections.[8–13] The innermost shell cross sections are available in tabular form.[14–16] Most of the measurements that have been made to date for both the K- and L-shell are for low atomic number projectiles ($Z_1 < 3$). There is also, however, a fairly large number of K- and L-shell production cross-section measurements for heavier incident ions. While a great deal of work has been devoted to K- and L-shell measurements, and some agreement between measurements at different laboratories has been found,[15,16] the limited number of studies that have been initiated on the more complex M-shell ionization shows considerable disagreement.

The earliest work on M-shell x ray yields was done half a century ago.[17–19] The determination of cross sections, however, started in the sixties, when flow mode proportional counters were being used.[20–23] More precise measurements, using high-resolution detectors, began to appear in the literature in the early 1970's.[24–27] Since then, the M-shell excitations have been investigated for a variety of ion-atom combinations, ion energies, and excitation mechanisms. The Si(Li) detector, crystal spectrometer, and photoelectron spectrometer have been some of the instruments employed in these studies.[28–43]

A closer look at $^{1}_{1}H^{+}$ and $^{4}_{2}He^{+}$ data for the M shell in the last decade shows that these studies are confined mostly to incident ion energies of 1 MeV/u or higher values,[23,26,28–31,36,38,39,41,43] producing a void in the experimental data for M-shell x-ray-production cross section at low velocities. In addition, the uncertainties quoted in these works are, for the most part, more than 25% and have been attributed to large errors in efficiency measurements or to large target thickness effects for which a correction had not been made.

The reasons for the difficulties associated with the M shell are due to the complexity of the M-shell spectrum. When an energetic ion passes through matter, the Coulomb interaction can produce ionization or excitation of inner-shell electrons of the target atoms. The resulting vacancies may be detected by observing characteristic x rays or Auger electrons. The number of transitions from higher shells which can fill an M-shell vacancy is much greater than would be for a K- or even an L-shell vacancy filling. Hence, there are more M-shell x rays than K- or L-shell x rays. Also, many of the transitions involved in the vacancy filling in the M

TABLE I. Target thicknesses.

Element	Z_2	Effective Thickness[a] ($\mu g/cm^2$)
Au	79	13.5
		23.2
Pb	82	9.92
		20.0
Bi	83	10.7
		21.2
U	92	15.0

[a]The target thicknesses given were measured with the target positioned in the beam at an angle of 45° with respect to the incident beam direction.

shell are overlapping in energy. Second, if measurements are made with the Si(Li) detector, there are uncertainties in the x-ray-production cross sections because of detector efficiency uncertainties at the low energies. This is owing to the lack of calibrated radioactive sources in this region.[44–51] The M-shell x rays of Au, Pb, Bi, and U, which we have studied, have energies in this uncertain region. Third, the K-shell x rays from the low-Z elements, which are contaminants in the target, are always present in the 1–5 keV range. These x rays give rise to the additional peaks that obscure an already complicated spectrum.

Khandelwal and Merzbacher[52] have provided the explicit form factors describing the energy loss and momentum transfer of a charged particle to electrons in the M subshells. Choi[53] extended this work in the plane-wave Born approximation (PWBA) to calculate the cross section for M-shell ionization for gold, uranium, and holmium atoms in collisions with protons. Johnson, Basbas, and McDaniel[54] further extended the theoretical work on M shell in the PWBA for direct ionization for other ion-target systems. Until the work of McGuire[55] on the M-shell Coster-Kronig, Auger, and radiative rates and fluorescence yields for Ca–Th, very few fluorescence yields were available to convert x-ray-production cross sections to ionization cross sections and to provide for a comparison of theory with experiment.

In the present paper we report the M-shell x-ray-production cross section for thin (~ 15 $\mu g/cm^2$, see Table I) targets of $_{79}$Au, $_{82}$Pb, $_{83}$Bi, and $_{92}$U for incident $^1_1H^+$ and $^4_2He^+$ ions. The energy of these projectiles ranged from 0.3 to 2.6 MeV. For the purpose of comparison, the M-shell ionization cross-section predictions of the first Born approximation, i.e., PWBA[54] for direct ionization plus the Oppenheimer-Brinkman-Kramers (OBK) of Nikolaev[56] for electron capture (OBKN) are converted to production cross sections using the single-hole fluorescence yields, Coster-Kronig transition rates and branching ratios.[55,57] The data are also compared with the theory by Brandt and Lapicki[58,59] that goes beyond the first Born approximation, i.e., the ECPSSR approach which accounts for the energy loss, Coulomb deflection, perturbed-stationary-state, and relativistic effects.

EXPERIMENTAL PROCEDURE

Ion beams of $^1_1H^+$ and $^4_2He^+$ were obtained from the 2.5-MV Van de Graaff accelerator at North Texas State University. The ion energy ranged from 0.3 to 2.6 MeV. The ion beams were energy and mass analyzed by a calibrated High-Voltage Engineering Corporation (HVEC) bending magnet. The analyzed beam was collimated by two 2-mm diameter tantalum apertures located 19 cm before the target chamber. The target was positioned at 45° to the incident beam direction. The scattered ions were monitored by a Si surface barrier detector at 150° while the x rays were counted by an ORTEC Si(Li) detector at 90° to the incident beam direction.

The targets used in the present experiment were prepared by the vacuum deposition of the elements $_{79}$Au, $_{82}$Pb, and $_{83}$Bi on an ultrapure carbon backing of thickness 15–20 $\mu g/cm^2$. A technique for production of ultrapure carbon foils was developed in the North Texas State University (NTSU) laboratory. The carbon foils were floated in an 80 °C solution of deionized distilled water and 30% acetone for an hour before being picked up on a steel frame. The carbon backings were screened for impurities by looking at the x rays produced by a 2.0-MeV protons incident on the carbon foil. The impurities of the elements $_{11}$Na through $_{20}$Ca have K-shell x rays in the region of the M-shell x rays of interest in the present study. Our technique was found to decrease the impurity level in the carbon foil by 50–75 %. The elemental layer of $_{79}$Au, $_{82}$Pb, and $_{83}$Bi was vacuum evaporated and deposited on the ultrapure carbon backing. The $_{92}$U targets were prepared by using an electron gun. The thickness of the elemental layer was determined by measuring Rutherford backscattering ions of ^1_1H and ^4_2He into a Si surface barrier detector. This detector was positioned at an angle of 150° to the incident beam direction. Several measurements, taken at 1.8, 2.0, and 2.2 MeV, were used to calculate an average value of the target thickness. Table I lists the measured average thicknesses. They have uncertainties of 1.5% due to counting statistics, source calibra-

tion, solid angle measurement, beam-energy uncertainty, and 3.5–7% uncertainty from nonuniformity of the elemental layer.

The ORTEC Si(Li) detector was positioned inside the target chamber with the 7.62-μm Be window 18.6 cm from the beam spot on the target. An Al collimator with a circular aperture of 5-mm diameter was interposed between the target and the Si(Li) detector to cut out x rays produced outside of the beam spot. The resolution of the Si(Li) detector was measured to be 160 eV at 5.9 keV.

The Si(Li) detector efficiency was determined by bombarding thin targets of low-Z elements with 2.0-MeV $^4_2$He ions. The resulting K-shell x-ray yield was normalized to the Rutherford scattered-particle yield, which was collected simultaneously with the x rays. The Rutherford cross section and the K-shell x-ray production from the ECPSSR theory[58] were used to determine the efficiency of the Si(Li) detector at that particular K-shell x-ray energy.[51] A calibrated source of ^{57}Co was used to determine the efficiency at 6.4 and 7.059 keV by procedures described in the literature.[44-51] In addition, a calculated efficiency curve was determined through the use of the manufacturer suggested values[60] for the thicknesses of Au contact layer (40 μg/cm^2), Si dead layer (0.5 μm), together with Be window thickness (7.62 μm) and the Mylar thickness (3.81 μm). The attenuation of the x rays in these various layers provided an attenuation curve. This curve was normalized to the measured ^{57}Co efficiency point at 6.4 keV to get the calculated efficiency curve. The efficiency of the Si(Li) detector is plotted versus the energy of the x rays in Fig. 1. The squares represent the efficiency determined from our K-shell x-ray measurement and the ECPSSR theory while the solid line is the efficiency curve calculated from

$$\epsilon=\epsilon_0 \exp\left[-\sum_i \mu_i x_i\right], \tag{1}$$

where x_i is the ith attenuation thickness, μ_i is the mass attenuation coefficient, and ϵ_0 is the efficiency in absence of any attenuator.

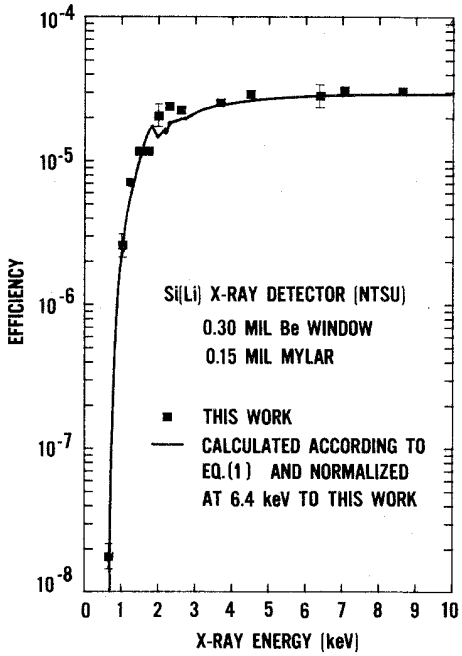

FIG. 1. Efficiency of the Si(Li) x-ray detector versus x-ray energy. This efficiency consists of the intrinsic efficiency of the Si(Li) detector and the solid angle subtended by the detector at this target position. Squares represent the efficiency determined from our measurements of the K x rays for low-Z elements. Squares at 6.4 and 7.059 keV represent the measurements with a ^{57}Co radioactive source. The 6.4 keV efficiency point is used to normalize the calculated curve shown by the solid line. The calculated efficiency curve was determined from Eq. (1) with the attenuation of the x rays in 3.81-μm Mylar, 7.62-μm Be window, the 40-μg/cm^2 Au contact layer, and the 0.5-μm Si dead layer of the detector.

The Si surface barrier detector at 150° was equipped with a 0.75-mm collimator to reduce the high count rate from the Rutherford scattered ions at low energies. The surface barrier detector, which had a full width at half maximum (FWHM) resolution of 13.3 keV, was calibrated for energy and solid angle using a calibrated ^{244}Cm source. The measured x-ray yield was normalized to the Rutherford scattering yield to determine the x-ray production cross section. Rutherford nature of the scattering was ensured by checking the ratio $E_1^2 Y/I$ for constancy where E_1 is the energy of the ion in MeV, Y is the scattered particle yield at 150°, and I is the charge collected in a Faraday cup. The Faraday cup was positioned behind the scattering chamber and collected the incident ion beam after it had passed through the thin targets.

The x-ray spectra from the Si(Li) detector and the Rutherford scattered particle spectra from the 150° surface barrier detector were stored in two 1024-channel multichannel analyzers. These spectra were transferred to a Tennecomp TP-50 lab computer system and were stored on a PDP 11-34 RL-01 hard disk. A 4096-channel histogram region on the TP-50 system allowed further analysis of the spectra.

DATA ANALYSIS

In Fig. 2, M-shell x-ray spectrum for 2-MeV $^1_1$H$^+$ on $_{92}$U is shown. The major peaks in the spectrum

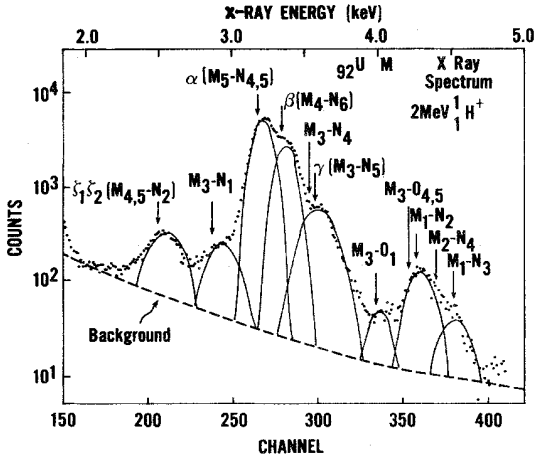

FIG. 2. An M x-ray spectrum of $_{92}$U for incident $^{1}_{1}H^{+}$ ions at 2.0 MeV. Channel numbers on the x axis at the bottom of the figure are converted to x-ray energies (in keV) at the top. The transitions involved in the M-shell x-ray spectrum are labeled and indicated by the arrows. A background spectrum, shown by a dashed curve, was subtracted from the spectrum. The subtracted yield, together with efficiency of the Si(Li) detector, is used to get a total M-shell x-ray-production cross section. Gaussian peaks represent the estimated shape, size, and position of some of the transitions.

are labeled by the transitions involved in the vacancy filling. The spectrum is seen to have three resolved peaks. The largest of these peaks is composed primarily of the M_α, M_β, and M_γ transitions. In Fig. 2, M_β is a shoulder on the M_α peak for $_{92}$U, while they appear as one peak in the $_{79}$Au, $_{82}$Pb, and $_{83}$Bi spectra. The M_γ peak appears as a shoulder on $M_{\alpha\beta}$ peak for all the targets. The determination of x-ray yield is done by fitting and subtracting a quadratic background spectrum and then finding the yield under the peaks. Since the various transitions are not resolved in this spectrum, a multi-Gaussian peak-fitting procedure is used. This nonlinear, least-square-fitting routine provides only estimates for the shape, size, and position for some of the transitions. Therefore, we present here only the total M-shell x-ray-production cross section and not the individual subshell x-ray-production cross sections.

The experimental M-shell x-ray-production cross section σ_{XM} is given by

$$\sigma_{XM}(b)=\sum_i \frac{Y_{XM_i}}{\epsilon_i}\frac{(d\sigma_R/d\Omega)d\Omega}{Y_R}\frac{\tau_x}{\tau_R}C_i\ , \quad (2)$$

where Y_{XM_i} is the yield under ith M x-ray peak, ϵ_i is

TABLE II. Experimental uncertainties.

Source	Range (%)
Relative uncertainty	
Counting statistics and background subtraction	
x-ray yields	1–4.5
Back-scattered particle yields	0.5–1.5
Uncertainty in x-ray yield due to uncertainty in incident energy[a]	0.1–6
Total relative uncertainty	<7.7
Normalization uncertainty	
Efficiency	6
Particle detector solid angle	3
Rutherford differential cross section through uncertainty in angle θ of particle detector ($\sim$2.5°)	5
Total normalization uncertainty	<8.4
Total absolute uncertainty	<11.4

[a]There was a 10-keV uncertainty in the energy. At lower energies the steepness of cross section with energy gives rise to large uncertainties at these energies. For $_2$He data, at 0.6, 0.5, 0.4, and 0.3 MeV, this uncertainty is 6.5, 9, 12 and 16% for U targets and 4, 6, 7, and 9% for Au, Pb, and Bi targets. For $_1$H data, at 0.5, 0.4, and 0.3 MeV, these percentages were 4, 5.6, and 8 for U targets, and 2.4, 3, and 4.5 for Au, Pb, and Bi targets.

the efficiency of the Si(Li) detector at the peak energy, $d\sigma_R/d\Omega$ is the differential Rutherford scattering cross section at the solid angle of 150°, $d\Omega$ is the solid angle of the 150° scattered particle detector, Y_R is the yield of Rutherford scattered particle, τ_x and τ_R are the corrections for dead time of the x-ray and the particle detector, respectively. The C_i represents the correction to the x ray and Rutherford yields to compensate for the energy loss of the ion in the finite thickness of the target.[61] The x-ray yield correction is $(1-\Delta E/E_1)^{-s}$, where E_1 is the incident energy of the ion and s is the slope of the natural logarithm of the cross section as a function of E_1. The Rutherford cross section varies inversely with the square of the energy and, therefore, the target thickness correction for the scattered particle yield is $(1-\Delta E_1/E_1)^{-2}$. For the thin targets used in this experiment, C_i in Eq. (2) was nearly unity. For the thickest uranium target used at the lowest energy, the target thickness correction was less than 0.5%. For $^4_2$He ions, the maximum correction was 3.7%. At all ion energies above 1 MeV, the target thickness correction was negligible.

Table II indicates the various uncertainties involved in the determination of these cross sections. X-ray yields are proportional to the ion energy raised to increasingly higher powers with decreasing projectile velocities. A 10-keV uncertainty in the incident energy affects the cross sections most strongly in the energy region below the 0.5-MeV helium on uranium data.

RESULTS AND DISCUSSION

The two primary modes of vacancy production in the target are (1) direct ionization to the target continuum (DI) and (2) electron capture to the projectile (EC). The first Born contributions of DI and EC to the target ionization cross section were calculated in the PWBA[54] and the OBKN[56] approximation, respectively. Calculations were also performed in the perturbed-stationary-state theory[58,59] which, in addition, accounts for the energy loss and Coulomb deflection of the projectile. These calculations account for perturbed stationary state and relativistic effects in the description of the M-shell electron. All of these effects are not accounted for in the first Born approximation.

In the present work, the EC contribution to the

TABLE III. Cross section for M-shell x-ray production by $^1_1H^+$ (cross sections are in barns).

Target / E(MeV)	$_{79}$Au	$_{82}$Pb	$_{83}$Bi	$_{92}$U
0.3	112	91.6	82.5	26.7
0.4	176	137	140	54
0.5	215	196	189	83.3
0.6	304	256	248	117
0.7	402	350	337	155
0.8	486	403	382	191
0.9	588	436	441	226
1.0	639	534	518	256
1.1	708	634	579	289
1.2	787	676	637	325
1.3	878	752	700	369
1.4	919	790	765	401
1.5	1010	884	874	433
1.6	1061	935	921	465
1.7	1162	1026	945	509
1.8	1246	1086	986	532
1.9	1285	1106	1028	566
2.0	1315	1254	1108	600
2.1	1378	1322	1174	688
2.2	1499	1371	1294	703
2.3	1524	1349	1204	727
2.4	1564	1426	1292	745
2.5	1604	1474	1393	762
2.6	1611	1478	1441	792

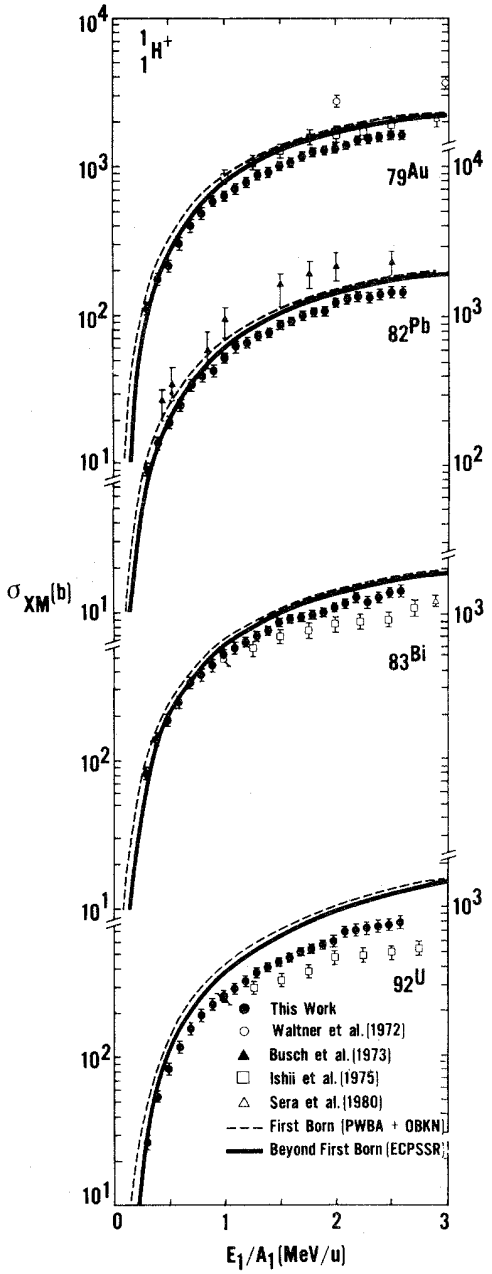

FIG. 3. *M*-shell x-ray-production cross sections of $_{79}$Au, $_{82}$Pb, $_{83}$Bi, and $_{92}$U for incident ions of $^1_1$H vs the projectile energy per its atomic mass. Present work is shown by solid circles. Measurements from Refs. 26, 28, 30, and 39 are also exhibited. In order to compare experimental data with theory, the predictions of two theories are plotted. Broken line represents the sum of the first Born calculations in the PWBA (Ref. 54) for DI and the OBKN (Ref. 56) for the EC to the total *M*-shell x-ray-production cross section. Solid curve represents the sum of DI and EC contributions to the total *M*-shell x-ray-production cross section according to the ECPSSR calculation (Refs. 58, 59).

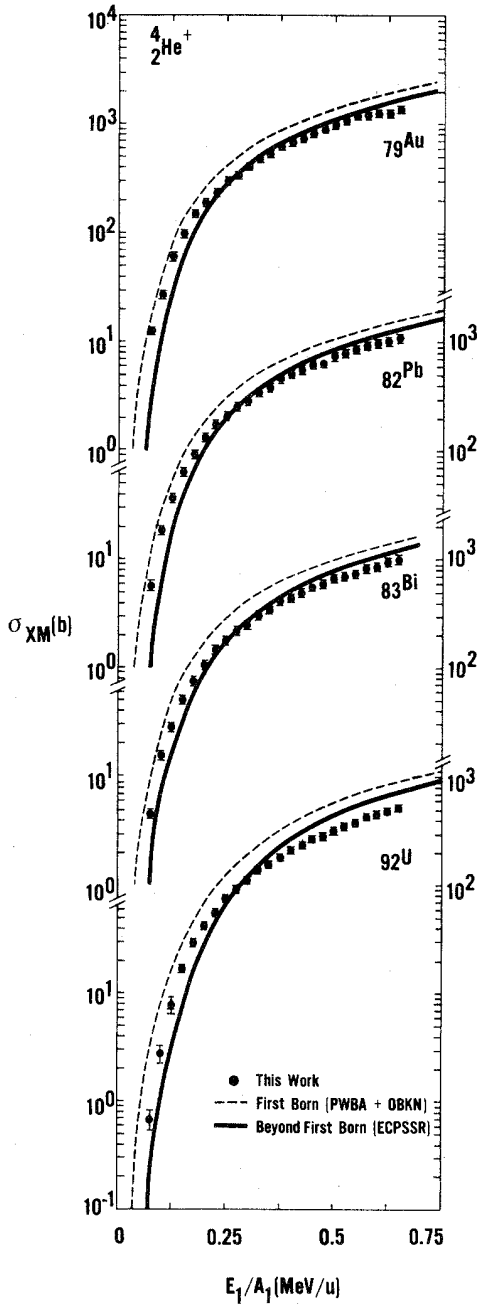

FIG. 4. *M*-shell x-ray-production cross sections of $_{79}$Au, $_{82}$Pb, $_{83}$Bi, and $_{92}$U for incident ions of $^4_2$He versus projectile energy per its atomic mass. Solid circles represent the present work. Broken line represents the sum of the first Born calculations in the PWBA (Ref. 54) for DI and the OBKN (Ref. 56) for the EC to the total *M*-shell x-ray-production cross section. Solid curve represents the sum of DI and EC contributions to the total *M*-shell x-ray-production cross section according to the ECPSSR calculation (Refs. 58,59).

total M-shell x-ray-production cross section was calculated in the OBKN approximation to be less than 8.0% for both $^1_1H^+$ and $^4_2He^+$ ion impact at all energies investigated. This contribution was calculated to be less than 3.4% in the ECPSSR approximation.[59] EC contributions increase with Z_1/Z_2 for the same velocity as they do for K- and L-shell ionization.[62–65]

The measured total M-shell x-ray-production cross section for incident ^1_1H and ^4_2He ions on targets of $_{79}Au$, $_{82}Pb$, $_{92}Bi$, $_{92}U$ are presented as a function of energy/u in Figs. 3 and 4, respectively. The experimental data are compared with the predictions of various ionization theories using single-hole fluorescence yields.[55,57] Tables III and IV list all cross sections measured in this work.

The two major experimental limitations in the accurate determination of these cross sections are (1) K-shell x-ray contamination from low-Z impurity elements and (2) lack of radioactive sources for efficiency determination of the Si(Li) detector at low energies (1–3 keV). These were partially overcome by (1) methods developed to produce ultraclean targets and by (2) measurement of the efficiency of the Si(Li) detector using K-shell x-ray yields from low-Z elements and the calculated K-shell x-ray-production cross section, a method suggested by Lennard and Phillips.[51]

The Si(Li) detector resolution limited the reporting of cross section to total M-shell x-ray-production cross section only. It would be very useful to take measurements in higher resolution (e.g., with x-ray crystal spectrometers) to resolve the overlapping transitions and allow comparisons with theoretical calculations for M-subshell ionization cross sections that have recently become available.[59]

In addition to the present work, experimental data from other investigations[26,28,30,39] are also shown. In Fig. 3, for the ^1_1H incident on $_{79}Au$, the data of Ishii *et al.*[30] and Sera *et al.*[39] lie above the present results and are in agreement with the ECPSSR calculations. The target used by Ishii *et al.*[30] was 342 $\mu g/cm^2$ while the Au target thickness used in the present experiment was 13.3 $\mu g/cm^2$. For both $_{83}Bi$ and $_{92}U$ targets, however, the data of Ishii *et al.*[30] are in agreement with our data at 1 MeV/u, but their results show smaller cross sections at higher energies than the present work and fall well below either theory. Again, their targets were much thicker than the targets in the

TABLE IV. Cross section for M-shell x-ray production by $^4_2He^+$ (cross sections are in barns).

E(MeV) \ Target	$_{79}Au$	$_{82}Pb$	$_{83}Bi$	$_{92}U$
0.3	12.7	5.7	4.55	0.67
0.4	27.3	18.3	15.3	2.73
0.5	60.6	36.1	28	7.7
0.6	97.8	63.4	50.5	16.8
0.7	150	91.9	74.8	29
0.8	191	132	106	41.4
0.9	238	174	146	54.6
1.0	302	208	179	74.6
1.1	341	254	221	91.4
1.2	405	287	251	111
1.3	484	343	305	137
1.4	532	379	346	155
1.5	630	456	412	180
1.6	681	507	446	209
1.7	741	555	504	233
1.8	809	626	563	265
1.9	887	649	603	287
2.0	975	748	678	321
2.1	1072	798	702	355
2.2	1177	862	748	382
2.3	1195	929	843	426
2.4	1248	988	873	455
2.5	1259	1034	969	477
2.6	1384	1107	1011	522

present work.

A comparison of the experimental M-shell x-ray-production cross section with those calculated from the existing first Born theories for the M-shell show that the sum of the PWBA + OBKN overpredicts almost all of the analyzed data at all energies for both ions. The ECPSSR calculations agree with the majority of the present data for both $^{1}_{1}$H and $^{4}_{2}$He ions at $\sim$0.35 MeV/u, overpredict the data at higher E_1/A_1 and underpredict the data at lower E_1/A_1. The overprediction increases with increasing MeV/u and increasing target Z_2. The disagreement between the data and the ECPSSR theory is also found to be greater for $^{4}_{2}$He data than $^{1}_{1}$H data at the same energy/u.

[1]T. B. Johansson, R. Akselsson, and S. A. E. Johansson, Nucl. Instrum. Methods 84, 141 (1970).

[2]K. R. Akselsson, IEEE Trans. Nucl. Sci. NS-28, 1370 (1981).

[3]L. J. Christensen, J. M. Khan, and W. F. Brunner, Rev. Sci. Instrum. 38, 20 (1967).

[4]T. J. Gray, R. Lear, R. J. Dexter, F. N. Schwettmann, and K. C. Weimer, Thin Solid Films 19, 103 (1973).

[5]B. D. Sartwell, A. B. Campbell III, B. S. Covino, Jr., T. J. Driscoll, IEEE Trans. Nucl. Sci. NS-26, 1670 (1979).

[6]B. M. Johnson, K. W. Jones, J. L. Cecchi, and T. H. Kruse, IEEE Trans. Nucl. Sci. NS-26, 1317 (1979).

[7]J. Kilwer and A. Elfiqi, IEEE Trans. Nucl. Sci. NS-26, 1323 (1979).

[8]G. Lapicki and A. R. Zander, Phys. Rev. A 23, 2072 (1981).

[9]J. J. Chmielewski, J. L. Flinner, F. W. Inman, B. Sollenberger, and N. V. Udeh, Phys. Rev. A 24, 29 (1981).

[10]M. Dost, S. Hoppenau, J. Kising, S. Röhl, and P. Schorn, Phys. Rev. A 24, 693 (1981).

[11]R. K. Rice, F. D. McDaniel, G. Basbas, and J. L. Duggan, Phys. Rev. A 24, 758 (1981).

[12]N. V. Udeh, J. J. Chmielewski, J. L. Flinner, F. W. Inman, and B. Sollenberger, Phys. Rev. A 24, 1746 (1981).

[13]J. Hall, P. Richard, T. J. Gray, C. D. Lin, K. Jones, B. Johnson, and D. Gregory, Phys. Rev. A 24, 2416 (1981).

[14]C. H. Rutledge and R. L. Watson, At. Data Nucl. Data Tables 12, 195 (1973); and T. L. Hardt and R. L. Watson, *ibid.* 17, 107 (1976).

[15]R. K. Gardner and T. J. Gray, At. Data Nucl. Data Tables 21, 515 (1978).

[16]H. Paul, At. Data Nucl. Data Tables, 24, 243 (1979); IEEE Trans. Nucl. Sci. NS-28, 1119 (1981).

[17]J. H. Williams, Phys. Rev. 37, 1431 (1931); 45, 71 (1934).

[18]H. Lay, Z. Phys. 91, 533 (1934).

[19]L. G. Parratt, Phys. Rev. 54, 99 (1938).

[20]R. C. Jopson, H. Mark, and C. D. Swift, Phys. Rev. A 127, 1612 (1962).

[21]J. M. Khan, D. L. Potter, and R. D. Worley, Phys. Rev. 135, A511 (1964); 136, A108 (1964); 139, A1735 (1965); 163, 81 (1967).

[22]R. C. Jopson, H. Mark, C. D. Swift, and M. A. Williamson, Phys. Rev. 137, A1353 (1965).

[23]P. B. Needham, Jr., and B. D. Sartwell, Phys. Rev. A 2, 27 (1970); 2, 1686 (1971).

[24]P. H. Mokler, Phys. Rev. Lett. 26, 811 (1971).

[25]P. H. Mokler, H. J. Stein, and P. Armbruster, Phys. Rev. Lett. 29, 827 (1972).

[26]A. W. Waltner, D. M. Peterson, G. A. Bissinger, A. B. Baskins, C. E. Busch, P. H. Nettles, W. R. Scates, and S. M. Shafroth, in *Proceedings of the International Conference on Inner Shell Ionization Phenomena and Future Applications, Atlanta, Georgia, 1972,* edited by R. W. Fink, S. T. Manson, J. M. Palms, and P. V. Rao, (U.S. Atomic Energy Commission, Oak Ridge, Tennessee, 1973), p. 1080.

[27]H. W. Schnopper, A. R. Sohwal, H. D. Betz, J. P. Delvaille, K. Kalata, K. W. Jones, and H. E. Wegner in Ref. 26, p. 1374.

[28]C. E. Busch, A. B. Baskin, P. H. Nettles, S. M. Shafroth, and A. W. Waltner, Phys. Rev. A 7, 1601 (1973).

[29]S. T. Thornton, R. H. McKnight, and R. R. Karlowicz, Phys. Rev. A 10, 219 (1974).

[30]K. Ishii, S. Morita, H. Tawara, H. Kaji, and T. Shiokawa, Phys. Rev. A 11, 119 (1975).

[31]V. S. Nikolaev, V. P. Petukhov, E. A. Romanovsky, V. A. Sergeev, I. M. Kruglova, and V. V. Beloshitsky, *The Physics of Electronic and Atomic Collisions* (University of Washington Press, Seattle, 1975), p. 419.

[32]C. L. Cocke, S. L. Varghese, J. A. Bedner, C. P. Bhalla, B. Curnutte, R. Kaufman, R. Randall, P. Richard, C. Woods, and J. H. Scofield, Phys. Rev. A 12, 2413 (1975).

[33]O. Keski-Rahkonen and M. O. Krause, Phys. Rev. A 15, 959 (1977).

[34]M. O. Krause, C. W. Nestor, Jr., and J. H. Oliver, Phys. Rev. A 15, 2335 (1977).

[35]D. E. Johnson, F. D. McDaniel, and G. Basbas, IEEE Trans. Nucl. Sci. NS-26, 1162 (1979).

[36]M. Poncet and Ch. Engelman, Nucl. Instrum. Methods 159, 455 (1979).

[37]D. H. H. Hoffman, C. Brendal, H. Genz, W. Löw, S. Müller, and A. Rühtu, Z. Phys. A 293, 187 (1979).

[38]H. J. Hay, J. Söderbaum, and P. B. Treacy, Nucl. Instrum. Methods 170, 261 (1980).

[39]K. Sera, K. Ishii, A. Yamadera, A. Kuwako, M. Kamiya, M. Sebata, S. Morita, and T. C. Chu, Phys. Rev. A

22, 2536 (1980).
[40]R. Mehta, J. L. Duggan, F. D. McDaniel, M. C. Andrews, R. M. Wheeler, R. P. Chaturvedi, P. D. Miller, and G. Lapicki, IEEE Trans. Nucl. Sci. NS-28, 1122 (1981).
[41]M. Sarkar, H. Mommsen, W. Sarter, and P. Schürkes, J. Phys. B 14, 3163 (1981).
[42]R. Mehta, F. D. McDaniel, J. L. Duggan, M. C. Andrews, P. D. Miller, L. A. Rayburn, and A. R. Zander, *Abstracts of the XII International Conference on the Physics of Electronic and Atomic Collisions, Gatlinburg, Tennessee, 1981,* edited by S. Datz (North-Holland, Amsterdam, 1981), p. 830.
[43]B. M. Johnson, D. C. Gregory, K. W. Jones, J. T. Sample, D. A. Hutcheon, R. Abegg, and G. J. Basbas in Ref. 42, p. 832.
[44]R. J. Gehrke and R. A. Lokken, Nucl. Instrum. Methods 97, 219 (1971).
[45]J. S. Hansen, J. C. McGeorge, D. Nix, W. D. Schmidt-Ott, I. Unus, and R. W. Fink, Nucl. Instrum. Methods 106, 365 (1973).
[46]J. L. Campbell and L. A. McNelles, Nucl. Instrum. Methods 117, 519 (1974).
[47]W. J. Gallagher and S. J. Cippola, Nucl. Instrum. Methods 122, 405 (1974).
[48]J. L. Campbell and L. A. McNelles, Nucl. Instrum. Methods 125, 205 (1975).
[49]G. Hubricht, B. Knaf, G. Presser, and J. Stähler, Nucl. Instrum. Methods 144, 359 (1977).
[50]D. Maor and B. Rosner, J. Phys. E 11, 1141 (1978).
[51]W. N. Lennard and D. Phillips, Nucl. Instrum. Methods 166, 521 (1979).
[52]G. S. Khandelwal and E. Merzbacher, Phys. Rev. 151, 12 (1966).
[53]B.-H. Choi, Phys. Rev. A 7, 2056 (1973).
[54]D. E. Johnson, G. Basbas, and F. D. McDaniel, At. Data Nucl. Data Tables 24, 1 (1979).
[55]E. J. McGuire, Phys. Rev. A 5, 1043 (1972).
[56]J. R. Oppenheimer, Phys. Rev. 31, 349 (1928); H. C. Brinkman and H. A. Kramers, Proc. Acad. Sci. (Amsterdam) 33, 973 (1930); V. S. Nikolaev, Zh. Eskp. Teor. Fiz. 51, 1263 (1966) [Sov. Phys.—JETP 24, 847 (1967)].
[57]J. H. Scofield, Phys. Rev. A 9, 1041 (1974).
[58]W. Brandt and G. Lapicki, Phys. Rev. A 23, 1717 (1981).
[59]G. Lapicki, Bull. Am. Phys. Soc. 26, 1310 (1981).
[60]ORTEC (private communication).
[61]R. Laubert, H. Haselton, J. R. Mowat, R. S. Peterson, and I. A. Sellin, Phys. Rev. A 11, 135 (1975).
[62]G. Lapicki and W. Losonsky, Phys. Rev. A 15, 896 (1977).
[63]F. D. McDaniel, J. L. Duggan, G. Basbas, P. D. Miller, and G. Lapicki, Phys. Rev. A 16, 1375 (1977).
[64]F. D. McDaniel, A. Toten, R. S. Peterson, J. L. Duggan, S. R. Wilson, J. D. Gressett, P. D. Miller, and G. Lapicki, Phys. Rev. A 19, 1517 (1979).
[65]G. Lapicki and F. D. McDaniel, Phys. Rev. A 22, 1896 (1980).